Hypoosmotic stress drives IL-33 production in human keratinocytes – a novel epidermal stress response

Wojciech Pietka[1,2], Denis Khnykin[1,2], Vibeke Bertelsen[2], Astrid Haaskjold Lossius[1,2], Tor Espen Stav-Noraas[1,2], Johanna Hol Fosse[1,2], Hilde Kanli Galtung[3], Guttorm Haraldsen[1,2,*] & Olav Sundnes[1,2,5]

[1]K.G.Jebsen Inflammation Research Centre, [2]Department of Pathology, [3]Department of Oral Biology, [5]Department of Rheumatology, Dermatology and Infectious Diseases, University of Oslo and Oslo University Hospital, Norway

*Correspondence: Guttorm Haraldsen, Department of Pathology, Oslo University Hospital Rikshospitalet, PO Box 4950 Nydalen, NO-0424 Oslo, Norway. Phone: (+47) 23 07 14 92 Fax: (+47) 23 07 15 11. E-mail: gharalds@rr-research.no

Short title: Hypoosmotic stress drives IL-33 expression

Abbreviations: IL-33, interleukin-33; IFN-γ, interferon gamma; EGF, epidermal growth factor

ABSTRACT

While inflammation has traditionally been considered a response to either exogenous pathogen-associated signals or endogenous signals of cell damage, other perturbations of homeostasis, generally referred to as stress, may also induce inflammation. The relationship between stress and inflammation is, however, not well defined. Here we describe for the first time a novel mechanism of interleukin-33 (IL-33) induction driven by hypoosmotic stress in human keratinocytes, and also reveal interesting differences when comparing responsiveness of other inflammatory mediators. The induction of IL-33 was completely dependent on EGFR- and calcium signaling, and inhibition of calcium signaling not only abolished IL-33 induction but also dramatically changed the transcriptional pattern of other cytokines upon hypoosmotic stress. IL-33 was not secreted but instead showed nuclear sequestration, conceivably acting as a fail-safe mechanism whereby it is induced by potential danger but only released upon more extreme homeostatic perturbations that result in cell death. Finally, stress-induced IL-33 was also confirmed in an *ex vivo* human skin model, translating this mechanism to a potential tissue-relevant signal in the human epidermis. In conclusion, we describe hypoosmotic stress as a novel mechanism of IL-33 expression, linking cellular stress to nuclear accumulation of a strong proinflammatory cytokine.

INTRODUCTION

Keratinocytes contribute to innate immune responses, activate antigen-presenting cells, and also direct lymphoid responses in the skin, bypassing conventional adaptive responses (Hayday, 2009). Despite increasing awareness of their importance in immune responses, the external stimuli driving keratinocyte activation are not yet fully defined. Keratinocytes express a wide range of pattern-recognition receptors with which they respond to exogenous microbial challenges or to endogenous molecules released during tissue injury (Nestle et al., 2009). In addition, they respond to a variety of cytokines produced by activated immune cells, resulting in inflammatory response modulation. Moreover, stressors such as hypoxia, generation of reactive oxygen or nitrogen species, heat shock and DNA damage may also affect keratinocyte immune function through homeostatic stress responses (Chovatiya and Medzhitov, 2014), but the exact nature of the relationship between stress and inflammatory responses is unclear.

The cellular stress response relies on cell-intrinsic adaptation and stress elimination. However, it also contains an important cell-extrinsic component that can alert adjacent cells and, if needed, induce an immune response (Chovatiya and Medzhitov, 2014). It is likely that different stimuli will trigger distinct epithelial mediator signatures that can shape the immune response according to the nature of stressors (Swamy et al., 2010).

The alarmin interleukin-33 (IL-33) has emerged as an important mediator of epithelial immune function (Palmer and Gabay, 2011). Upon synthesis, IL-33 resides in the nuclei of epithelial, endothelial and stromal cells, and is hidden from the immune system until release from damaged cells (Haraldsen et al., 2009). A large body of experimental models has demonstrated important roles for IL-33 in inflammation, especially at epithelial surfaces

(Palmer and Gabay, 2011) where innate lymphoid cells and mast cells appear to be the main target cells (Molofsky et al., 2015). Although much of the literature considers IL-33 to be constitutively expressed in the mammalian skin, we challenge this view with our recent report of substantial species differences, pointing out that levels of IL-33 in normal human epidermis are low or undetectable (Sundnes et al., 2015), and that induction of human IL-33 is a response to pro-inflammatory signals rather than a constitutive property of the epidermis.

IFN-γ is the best characterized inducer of IL-33 in human keratinocytes (Meephansan et al., 2012; Seltmann et al., 2013; Sundnes et al., 2015). We expand this knowledge by reporting that hypoosmotic stress is also a strong inducer of IL-33, independent of JAK-signaling but, like the IFN-γ -response, dependent on EGFR- and calcium-signaling. We also report that, different sets of keratinocyte-derived cytokines were subject to distinct patterns of osmoregulation and responsiveness to calcium signaling. Hypoosmotic stress-induced IL-33 expression was also confirmed in the human epidermis by *ex vivo* skin organ culture.

RESULTS

Hypoosmotic stress induces IL-33 expression in primary human keratinocytes

We recently reported strong IL-33 induction in basal keratinocytes during human skin wounding (Sundnes et al., 2015). Based on our observation that IFN-γ drives expression of IL-33 in *ex vivo* organ cultures, we assessed STAT1-phosphorylation (pSTAT1) as a marker of IFN-γ activity in wound lesions, only to discover that such phosphorylation was undetectable despite strong induction of IL-33 (Fig 1a&b). We therefore hypothesized that other pathways may regulate IL-33 expression in keratinocytes and evaluated the ability of different stressors to modulate IL-33. Among several stress conditions tested, including acidic or oxidative stress, as well as heat shock, we found that IL-33 synthesis was strongly induced upon hypoosmotic stress (145 mOsm, Fig 1c-e), yet detected no IL-33 protein in the growth medium (data not shown). Immunofluorescent staining showed a strong nuclear signal but no evidence of cytoplasmic IL-33 (Fig 1d). Induction of IL-33 was restricted to hypoosmotic stress and not observed under hyperosmotic conditions, irrespective of ionic (addition of NaCl, Fig 1e) or non-ionic (addition of sorbitol, data not shown) stress. These findings were confirmed at the mRNA level, indicating transcriptional regulation (Fig 1f). Western blot data of cellular lysates demonstrated presence of full-length (31k Da) IL-33 that disappeared after transfection with IL-33 specific siRNA (Fig 1g) and revealed no evidence of shorter cleavage products. We also assessed whether hypoosmotic stress affected IL-33 expression in quiescent endothelial cells (that unlike keratinocytes show strong constitutive expression of IL-33, (Küchler et al., 2008)) and detected a weak but consistent enhancement of IL-33 expression upon hypoosmotic stress (Supplementary Figure S1a).

The epithelial chemokine interleukin-8 (IL-8) responds to both hypo- and hyperosmotic stress in Caco-2 cells (Hubert et al., 2004). This difference between IL-8 and IL-33 regulation

indicates that osmotic stress response mechanisms might differ according to the class and targets of cytokines. To test this hypothesis, we examined a selection of keratinocyte-derived immune mediators. First, we confirmed that IL-8 expression was also increased by both hyper- and hypoosmotic stress in human keratinocytes (Fig 1h). Second, we observed that the CXCR3-ligand CXCL11, which like IL-33 is induced upon IFN-γ stimulation (Klunker et al., 2003) and also CCL20, another T cell-recruiting chemokine, were also upregulated by hypoosmotic but not by hyperosmotic stress (Fig 1i&j). Finally, and by contrast, CXCL2 and IL-1α showed an opposite expression pattern, with upregulation by hyperosmotic stress only (Fig 1k&l), whereas TSLP, another activator of innate lymphoid cells, was insensitive to any modulation of osmolarity (data not shown). These profiles reveal that inflammatory cytokines are distinctly regulated in response to osmotic stress.

Prolonged hypotonic membrane stretch is required to induce IL-33 expression

Within minutes of exposure to hypoosmotic stress, keratinocytes showed an atypical morphology with membrane blebbing (Fig 2a, Supplementary Figure S2a). Blebbing occurs when an increase in intracellular pressure causes increased tension on the cytoskeleton and detachment of the plasma membrane from the underlying actin filaments (Lulevich et al., 2010). Indeed, similar massive membrane blebbing was observed within seconds during keratinocyte exposure to the actin polymerization inhibitor latrunculin A in isoosmotic medium, a condition that nevertheless failed to induce IL-33 expression, (Supplementary Figure S2b-f). Moreover, the presence of latrunculin A did not prevent the IL-33 induction observed upon exposure to hypoosmotic medium (Supplementary Figure S2e&g), indicating that an intact actin cytoskeleton is not essential for the signal transduction leading to IL-33 upregulation upon hypoosmotic stress.

To further explore this phenomenon, we exposed cells to hypoosmotic medium for a range of time points before changing back to normal medium. We found that prolonged hypoosmotic exposure for at least 5 hours was required for IL-33 induction (Fig 2b), indicating that either a prolonged reduction in ion concentrations or prolonged membrane stretch due to hypotonic cell swelling activated the response. To explore the effect of either mechanism, we first substituted main ionic components of the medium (sodium and chloride) by dilution of the medium with isosmotic solutions of sodium gluconate (replacing 50% of Cl^-) or potassium gluconate (replacing 50% of Na^+ and Cl^-) and revealed that hypoosmotic conditions *per se* were necessary, rather than reduced levels of Na^+ and Cl^- (Fig 2c). To confirm that cell swelling due to hypotonicity is sufficient for IL-33 induction, cells were exposed to isoosmotic medium where 50% was replaced by an isoosmotic urea-solution. As urea can cross the cell membrane relatively freely through facilitated diffusion, such conditions will cause cell swelling despite isoosmolarity. Indeed, urea solution caused massive blebbing and IL-33 induction, similar to hypoosmotic stress condition, as opposed to control cells exposed to an isoosmotic sorbitol-solution (non-membrane permeable osmolyte) (Fig 2d&e).

In most cells types, the acute exposure to hypoosmotic conditions drives a rapid cell volume increase within minutes, followed by a regulatory volume decrease (RVD). The keratinocyte-specific morphological response of blebbing made it difficult to directly address the role of the RVD in IL-33 regulation. However, the prolonged hypoosmotic exposure needed to induce IL-33 makes it unlikely that the response is driven by RVD alone. Given the recent report that RVD could activate the inflammasome in macrophages, leading to IL-1β release (Compan et al., 2012), we also pre-incubated keratinocytes with two different caspase-1 inhibitors prior to hypoosmotic stimulation but observed no effect to indicate caspase-1 involvement in IL-33 induction (Supplementary Figure S2h&i).

Stress-induced expression of IL-33 depends on EGFR signaling and has upstream mediators that differ from those of IFN-γ-mediated induction.

We recently reported that EGFR signaling was required but not sufficient to induce IL-33 during IFN-γ treatment (Sundnes et al., 2015). We observed a similar dependency in the hypoosmotic response, because EGFR inhibition (Fig 3a) or removal of EGFR ligands from the growth medium prevented induction of IL-33, while it was rescued by addition of the EGFR-ligand amphiregulin (Fig 3b).

To further compare IFN-γ and hypoosmotic induction we studied IL-33 expression at the single cell level by immunocytochemistry. As described by us elsewhere (Sundnes et al., 2015), only a small subset of keratinocytes expressed nuclear IL-33 in the basal state (Fig 3c). Further analyses revealed that most IL-33+ cells were Ki67-negative, i.e. not proliferating (Fig 3f), and that IFN-γ treatment predominantly boosted IL-33 expression in non-proliferating cells (Fig 3d&g). By contrast, hypoosmotic stress induced IL-33-expression in most cells and included the proliferating, Ki67-positive population (Fig 3e&h). These results indicated a difference in the upstream cellular signaling induced by the two stimuli, despite the common dependence on EGFR signaling. To underscore this difference, we assessed the involvement of Janus kinases (JAK), observing that pre-incubation with a pan-JAK inhibitor (JAK inhibitor I) dose-dependently abolished IL-33 induction by IFN-γ, but not that of hypoosmotic stress (Fig 3i).

Calcium-dependent processes drive IL-33 production and direct the general pro-inflammatory response to hypoosmotic stress

Hypoosmotic stress is known to induce calcium transients in a wide variety of cells, including keratinocytes (Azorin et al., 2011; Hoffmann et al., 2009). To examine whether IL-33 induction depends on calcium signaling, we preincubated keratinocytes with BAPTA-AM, a cell-permeable calcium chelator, and found that it completely abolished IL-33 protein synthesis during hypoosmotic stress or exposure to IFN-γ (Fig 4a). To determine whether this response was dependent on intracellular calcium stores or influx of extracellular calcium we chelated both intracellular and extracellular (BAPTA-AM) or only extracellular (EGTA) calcium ions. EGTA exposure resulted in a partial inhibition, while BAPTA-AM led to complete inhibition of IL-33 induction (Fig 4b), suggesting that both release from intracellular ER/Golgi stores and entry of extracellular calcium are involved.

The growth medium used in our experiments has a low calcium concentration. We therefore assessed the effect of hypoosmolarity in a high-calcium setting (1.2 mM) and observed only a slightly enhanced IL-33 response (Fig 4b). On the other hand, differentiating cells in high calcium-medium did not increase but rather tended to decrease IL-33 expression (Supplementary Figure S3a&b), excluding the possibility of calcium-dependent differentiation processes driving IL-33 expression.

Calcium is a crucial second messenger for a wide range of cellular processes (Berridge et al., 2000) and is involved in keratinocyte differentiation and migration (Vandenberghe et al., 2013). Time-lapse microscopy revealed that pre-incubation with BAPTA-AM for 30 min prior to hypoosmotic medium exposure abolished typical changes in keratinocytes

morphology occurring during hypoosmotic stress (Supplementary Figure S3c), with minimal membrane blebbing and no apparent swelling.

The completely different morphology and behavior of BAPTA-AM-treated cells upon hypoosmotic stress led us to ask whether calcium depletion also affects the expression of other pro-inflammatory cytokines. As expected, the *IL33* was completely inhibited by calcium chelation (Fig 4c, Supplementary Figure S3d). Moreover, the CXCR3 ligands *CXCL10* & *CXCL11* were partially inhibited, whereas, unexpectedly, the other mediators (*IL8*, *CCL20*, *CXCL2* and *IL1A*) showed completely opposite responses (Fig 4c, Supplementary Figure S3e-j). *IL8* and *CCL20* were induced upon hypoosmotic stress and showed a strongly exaggerated response upon simultaneous calcium chelation (Fig 4c, Supplementary Figure S3g&h). Even more striking, *CXCL2* and *IL1A*, which are not induced upon hypoosmotic stress alone, showed strong induction upon simultaneous calcium chelation (Fig 4c, Supplementary Figure S3i&j).

IL-33 is a nuclear protein and a putative transcriptional repressor, but its intracellular effects are not yet fully elucidated. Meephansan et. al previously showed that IL-33 knockdown could potentiate TNF-α-induced IL-8 production in keratinocytes, implicating IL-33 in regulation of gene transcription in keratinocytes (Meephansan et al., 2012). We therefore asked whether IL-33 itself could be the calcium-dependent factor that dampens the transcription of other cytokines during hypoosmotic stress. However, knockdown of IL-33 failed to increase mRNA levels of either IL-8 or CXCL2, while *IL1A* expression was only marginally increased (Fig 4d), ruling out that intracellular IL-33 is a major contributor in this setting.

Next, we investigated upstream events of calcium signaling leading to IL-33 induction and found that IL-33 upregulation was independent of store-operated calcium entry channel Orai1 and calcium sensor STIM1 (Supplementary Figure S4a&b). Moreover, TRP channels, L-type voltage gated calcium channels, purinergic receptors and PLC-γ were all redundant for IL-33 induction (Supplementary Figure S4c-f).

Hypoosmotic stress is a relevant tissue signal

To confirm that hypoosmotic stress constitutes a relevant signal in the tissue setting, we took advantage of a skin organ culture model. Skin samples fixed immediately after harvest showed, in agreement with previous observations, low IL-33 expression in epidermis but prominent expression in dermal endothelial cells (Fig 5a). Incubation in normal medium for 24 hours resulted in no induction of IL-33 in the epidermis but gave a reduction in endothelial IL-33 (Fig 5b). By contrast, a strong nuclear induction of epidermal IL-33 was observed after incubation for 24 hours in hypoosmotic medium (Fig 5c). Unlike IFN-γ stimulation (Fig 5d), this response was not associated with increased pSTAT1, thus mirroring the conditions observed during wound healing *in vivo*.

DISCUSSION

Cell swelling induced by hypoosmotic stress has been proposed as a conserved danger signal in several recent publications. At the single cell level, swelling activates the NLRP3 inflammasome in macrophages (Compan et al., 2012), explaining earlier observations that they secrete IL-1β when exposed to hypoosmotic medium (Perregaux et al., 1996). At the level of a whole organism, a drop in interstitial osmotic pressure upon wounding in the freshwater habitat of zebrafish, initiates eicosanoid-driven leukocyte recruitment (Enyedi et al., 2013). Moreover, osmotic surveillance mediated effective wound closure by epithelial cells in the same model through an ATP-dependent mechanism (Gault et al., 2014). Together these findings link non-lethal cellular/tissue stress to an inflammatory and regenerative response. Others have used the term 'homeostatic danger signals' for processes that do not result directly from pathogens or from dying or damaged cells (Gallo and Gallucci, 2013), as well as the recently introduced term 'homeostasis-altering molecular processes' (HAMPs, (Liston and Masters, 2017).

The role of hypoosmotic cell swelling *in vivo* in mammals is less clear. We reveal here that IL-33 induction occurs upon hypoosmotic stress not only in submerged cell culture but also in *ex vivo* cultured human skin. In addition, we made efforts to reproduce this response *in vivo* in a healthy human volunteer by injecting a bolus of sterile water intradermally and using isosmotic saline as a control. We found that this failed to induce epidermal IL-33 (unpublished observations). We believe that a single injection is unlikely to produce the sufficiently prolonged hypoosmotic stimulus that we show to be required for IL-33 induction *in vitro*. An interesting observation from the experiment is nevertheless that sterile water injection produced pain and later visible erythema, revealing increased infiltration of neutrophils when compared to saline injection (unpublished data). This experiment thus

confirms that brief hypoosmotic stress indeed initiates an inflammatory response *in vivo*, although not causing an epidermal IL-33 induction.

Whether the very low osmolarity explored as a model condition in this study actually occurs in human skin physiology and pathophysiology is questionable, but it is worth mentioning that the common vertebrate extracellular osmolarity (270-300 mOsm) differs substantially from that of saliva (~30 mOsm) in the mouth and oesophagus (Gault et al., 2014), perhaps contributing to the more rapid regeneration of wounds in the oral cavity. It is also likely that tissues experience prolonged smaller variations in osmolarity, which could be a relevant stress signal *in vivo*. An interesting observation, as commented by others (Kippenberger et al., 2005), is that exposure to freshwater tends to aggravate eczema and atopic dermatitis. In this pathophysiological context (i.e. eczema lesions) there is most likely a reduced epidermal barrier function that may render the epidermis more sensitive to external osmotic stress.

A more important pathophysiological relevance of the hypoosmotic response may be the cell swelling that occurs upon reversible cell damage (Kroemer et al., 2008), also known as hydropic swelling. This cell response is not a result of altered extracellular osmolarity but rather the impaired function of cell membranes and ion pumps. A wide range of stimuli can cause reversible cell damage either directly to the plasma membrane or indirectly by affecting the function of ion transporters, e.g. ATP depletion upon hypoxia. The net result of such damage is that the cell no longer maintains the normal ionic gradient across the cell membrane, leading to accumulation of intracellular Na+ and subsequent osmotic swelling due to water influx. In this manner, hypoosmotic conditions can mimic events that occur upon non-lethal cell damage. We have previously published that IL-33 was strongly induced at the wound edge in a human *in vivo* model (Sundnes et al., 2015). Here we show that the

response was likely independent of IFN-γ, as there was no detectable pSTAT1 signal at the wound edge. It is thus tempting to speculate that increased IL-33 expression upon human skin wounding is mediated through damage-induced cell swelling. There are also several acute skin conditions, such as erythema multiforme and drug eruptions, that are characterized histologically by hydropic degeneration of basal keratinocytes, but there currently are no reports on skin expression pattern of IL-33 in these settings.

Interestingly, we could not detect cell swelling *per se* in hypoosmotically stressed human primary keratinocytes *in vitro*. Rather, we show that their strong cytoskeleton contained the increase in intracellular pressure for some time but that it eventually resulted in massive membrane blebbing. This finding has implications for studying the hypoosmotic responses in cultured keratinocytes and to our knowledge it has not been addressed before.

Others have shown in rodents that IL-33 can be induced by mechanical strain in fibroblasts and by pressure overload in endothelial cells (Chen et al., 2015; Kakkar et al., 2012; Sanada et al., 2007). This represents a different type of mechanical stress experienced *in vivo* by endothelial cells and fibroblasts of the vasculature. The relationship between mechanical strain and osmotic swelling is unclear, but it would be reasonable to assume that common signaling cascades might be involved. However, at least in the fibroblasts, IL-33 was reported to be continuously secreted from living cells while we could not detect IL-33 in the culture medium (data not shown) despite robust and sensitive detection by ELISA in cell lysates.

As IL-33 does not appear to be secreted from keratinocytes, but rather accumulates in the nuclear compartment, it begs the question whether IL-33 participates in the homeostatic response as a nuclear factor. Although others have shown that intracellular IL-33 can affect

the inflammatory response (Ali et al., 2011; Meephansan et al., 2012), suppression of IL-33 did not have a marked effect on the inflammatory mediators tested in our study. One possibility is that IL-33 is involved in non-immune homeostatic responses and future global transcriptome analyses should address this question. Yet another possibility is that IL-33 is simply stored in the nucleus to prevent immune activation until needed further. In both cases the induction will effectively be a fail-safe mechanism, whereby IL-33 production is induced upon perturbation of homeostasis and will only be released if homeostasis is not restored and the cell is damaged or necrotic. Importantly, IL-33 is inactivated by apoptotic caspases thus preventing unnecessary immune activation upon non-inflammatory programmed cell death (Lüthi et al., 2009).

In this study we found that calcium signaling is crucial for IL-33 induction. Calcium is a ubiquitous intracellular messenger, and its important role is reflected by the myriad of regulating elements including pumps, channels, sensors, binding proteins and receptors. Keratinocytes are unique in that they proliferate in calcium concentrations below 0.1 mM and that concentrations above this level induce a differentiated phenotype. In fact, the epidermis maintains a calcium gradient across the cell layers reflecting this important concept (Mascia et al., 2012). The roles of calcium signaling in the immune functions of keratinocytes are less well described. A recent publication suggest that Orai1/ Nuclear factor of activated T-cells (NFAT) calcium signaling is essential for TSLP secretion in keratinocytes (Wilson et al., 2013). In our study we describe an effect that is distinct from this pathway as neither blocking of store operated Ca^{2+} entry (SOCE) or NFAT (by FK506, data not shown) attenuated the IL-33 production. Although we cannot yet explain the exact mode of calcium release, it appears that calcium signaling is crucial in shaping the immune activation of

keratinocytes, as chelating intracellular calcium completely changed the pattern of stress-induced cytokine production.

In conclusion, we show that IL-33 is strongly induced upon hypoosmotic stress, demonstrating, to our knowledge, for the first time a stress-induced regulation of this cytokine in keratinocytes. We also show different patterns of cytokine production in keratinocytes that is dependent on the osmotic conditions of the milieu. Moreover, we describe intriguing calcium-dependent processes that direct cytokine response to cellular stress. Defining these inflammatory pathways and mechanisms that modulate expression of stress-induced cytokines such as IL-33 could unravel novel therapeutic targets.

MATERIALS AND METHODS

Reagents

Recombinant human IFN-γ, EGF and amphiregulin from R&D Systems (Minneapolis, MN), AG1478, nifedipine, apyrase, Ruthenium Red, GRGDSP (RGD peptide), EGTA, potassium gluconate, sodium gluconate, urea and D-sorbitol from Sigma (St. Louis, MO), ML-9 and U73122 from Tocris (Bristol, UK), BAPTA-AM from LifeTechonolgies, PP1, PP2, Jak inhibitor I and verapamil from Calbiochem (now Merck Millipore), Z-WEHD-FMK and latrunculin A from Enzo Life Sciences, Caspase inhibitor IV from Santa Cruz and cetuximab from Merck Serono (Darmstadt, Germany). Other antibodies are listed in the supplementary table.

Human tissues

Human tissue was obtained in accordance with the Declaration of Helsinki and protocols approved by the Regional Committee for Research Ethics. Abdominal and breast skin samples were obtained during plastic surgery from Caucasian females aged 30-55. The human skin wound model was performed on a male Caucasian volunteer and has been described previously (Sundnes et al., 2015).

Cell culture

Pooled (n>3 donors) primary human neonatal keratinocytes (CELLnTEC, Switzerland), were grown in serum-free proliferation medium (CnT-57, CELLnTEC, Switzerland). Cells were split before reaching confluence and all experiments were performed at passage 3-6. Within each experiment 3 replicates (i.e. cells coming from the same batch) were treated identically.

Calcium-free CnT-57 was used for low calcium conditions and for high calcium conditions 1.2 mM of $CaCl_2$ (Sigma) was added.

Statistics

Data are presented as mean ± SD of three replicates taken from one independent experiment, unless stated otherwise. Each experiment was repeated independently 3 times. Differences between means were calculated by one-way ANOVA with Tukey's multiple comparison tests by using GraphPad Prism 6 software (GraphPad Software, La Jolla, CA), $P<0.05$ was considered statistically significant.

CONFLICT OF INTERESTS

None

ACKNOWLEDGEMENTS

We thank Aaste Aursjø, Sara Halmøy Bakke, Kathrine Hagelsteen, Kjersti Thorvaldsen Hagen, Danh Phung and Linda Solfjell for excellent technical assistance and the Aleris Colosseum clinic for providing skin tissue. We thank Manuela Zucknick at the Oslo Center for Biostatistics and Epidemiology for support with statistical analyses.

REFERENCES

Ali, S, Mohs, A, Thomas, M, Klare, J, Ross, R, Schmitz, ML, *et al.* (2011). The dual function cytokine IL-33 interacts with the transcription factor NF-κB to dampen NF-κB-stimulated gene transcription. *J Immunol* 187: 1609–16.

Azorin, N, Raoux, M, Rodat-Despoix, L, Merrot, T, Delmas, P, Crest, M, (2011). ATP signalling is crucial for the response of human keratinocytes to mechanical stimulation by hypo-osmotic shock. *Exp Dermatol* 20: 401–7.

Berridge, MJ, Lipp, P, Bootman, MD (2000). The versatility and universality of calcium signalling. *Nat Rev Mol Cell Biol* 1: 11–21.

Chen, W-Y, Hong, J, Gannon, J, Kakkar, R, Lee, RT (2015). Myocardial pressure overload induces systemic inflammation through endothelial cell IL-33. *Proc Natl Acad Sci USA* 201424236.

Chovatiya, R, Medzhitov, R (2014). Stress, inflammation, and defense of homeostasis. *Mol Cell* 54: 281–8.

Compan, V, Baroja-Mazo, A, López-Castejón, G, Gomez, AI, Martínez, CM, Angosto, D, *et al.* (2012). Cell volume regulation modulates NLRP3 inflammasome activation. *Immunity* 37: 487–500.

Enyedi, B, Kala, S, Nikolich-Zugich, T, Niethammer, P (2013). Tissue damage detection by osmotic surveillance. *Nat Cell Biol* 15: 1123–30.

Gallo, PM, Gallucci, S (2013). The dendritic cell response to classic, emerging, and homeostatic danger signals. Implications for autoimmunity. *Front Immunol* 4: 138.

Gault, WJ, Enyedi, B, Niethammer, P (2014). Osmotic surveillance mediates rapid wound closure through nucleotide release. *J Cell Biol* 207: 767–82.

Grøvdal, LM, Stang, E, Sorkin, A, Madshus, IH (2004). Direct interaction of Cbl with pTyr 1045 of the EGF receptor (EGFR) is required to sort the EGFR to lysosomes for degradation. *Exp Cell Res* 300: 388–95.

Haraldsen, G, Balogh, J, Pollheimer, J, Sponheim, J, Küchler, AM (2009). Interleukin-33 - cytokine of dual function or novel alarmin? *Trends Immunol* 30: 227–33.

Hayday, AC (2009). Gammadelta T cells and the lymphoid stress-surveillance response. *Immunity* 31: 184–96.

Hoffmann, EK, Lambert, IH, Pedersen, SF (2009). Physiology of cell volume regulation in vertebrates. *Physiol Rev* 89: 193–277.

Hubert, A, Cauliez, B, Chedeville, A, Husson, A, Lavoinne, A (2004). Osmotic stress, a proinflammatory signal in Caco-2 cells. *Biochimie* 86: 533–41.

Kakkar, R, Hei, H, Dobner, S, Lee, RT (2012). Interleukin 33 as a mechanically responsive cytokine secreted by living cells. *J Biol Chem* 287: 6941–8.

Kippenberger, S, Loitsch, S, Guschel, M, Müller, J, Kaufmann, R, Bernd, A (2005). Hypotonic stress induces E-cadherin expression in cultured human keratinocytes. *FEBS Lett* 579: 207–14.

Klunker, S, Trautmann, A, Akdis, M, Verhagen, J, Schmid-Grendelmeier, P, Blaser, K, *et al.* (2003). A second step of chemotaxis after transendothelial migration: keratinocytes undergoing apoptosis release IFN-gamma-inducible protein 10, monokine induced by IFN-gamma, and IFN-gamma-inducible alpha-chemoattractant for T cell chemotaxis toward epidermis in atopic dermatitis. *J Immunol* 171: 1078–84.

Kroemer, G, Galluzzi, L, Vandenabeele, P, Abrams, J, Alnemri, ES, Baehrecke, EH , *et al.* (2008). Classification of cell death: recommendations of the Nomenclature Committee on Cell Death 2009. *Cell Death Differ* 16: 3–11.

Küchler, AM, Pollheimer, J, Balogh, J, Sponheim, J, Manley, L, Sorensen, DR, *et al.* (2008). Nuclear interleukin-33 is generally expressed in resting endothelium but rapidly lost

upon angiogenic or proinflammatory activation. *Am J Pathol* 173: 1229–42.
Liston, A, Masters, SL (2017). Homeostasis-altering molecular processes as mechanisms of inflammasome activation. *Nat Rev Immunol* 17: 208–14.
Lulevich, V, Yang, H-Y, Isseroff, RR, Liu, G-Y (2010). Single cell mechanics of keratinocyte cells. *Ultramicroscopy* 110: 1435–42.
Lüthi, AU, Cullen, SP, McNeela, EA, Duriez, PJ, Afonina, IS, Sheridan, C, *et al.* (2009). Suppression of interleukin-33 bioactivity through proteolysis by apoptotic caspases. *Immunity* 31: 84–98.
Mascia, F, Denning, M, Kopan, R, Yuspa, SH (2012). The black box illuminated: signals and signaling. *J Invest Dermatol* 132: 811–9.
Meephansan, J, Tsuda, H, Komine, M, Tominaga, S-I, Ohtsuki, M (2012). Regulation of IL-33 Expression by IFN-γ and Tumor Necrosis Factor-α in Normal Human Epidermal Keratinocytes 132: 2593–600.
Molofsky, AB, Savage, AK, Locksley, RM (2015). Interleukin-33 in Tissue Homeostasis, Injury, and Inflammation. *Immunity* 42: 1005–19.
Nestle, FO, Di Meglio, P, Qin, J-Z, Nickoloff, BJ (2009). Skin immune sentinels in health and disease. *Nat Rev Immunol* 9: 679–91.
Palmer, G, Gabay, C (2011). Interleukin-33 biology with potential insights into human diseases. *Nat Rev Rheumatol* 7: 321–9.
Perregaux, DG, Laliberte, RE, Gabel, CA (1996). Human monocyte interleukin-1beta posttranslational processing. Evidence of a volume-regulated response. *J Biol Chem* 271: 29830–8.
Sanada, S, Hakuno, D, Higgins, LJ, Schreiter, ER, McKenzie, ANJ, Lee, RT (2007). IL-33 and ST2 comprise a critical biomechanically induced and cardioprotective signaling system. *J Clin Invest* 117: 1538–49.
Seltmann, J, Werfel, T, Wittmann, M (2013). Evidence for a regulatory loop between IFN-γ and IL-33 in skin inflammation. *Exp Dermatol* 22: 102–7.
Sundnes, O, Pietka, W, Loos, T, Sponheim, J, Rankin, AL, Pflanz, S, *et al.* (2015). Epidermal Expression and Regulation of Interleukin-33 during Homeostasis and Inflammation: Strong Species Differences. *J Invest Dermatol*.
Swamy, M, Jamora, C, Havran, W, Hayday, A (2010). Epithelial decision makers: in search of the 'epimmunome'. *Nat Immunol* 11: 656–65.
Vandenberghe, M, Raphaël, M, Lehen'kyi, V, Gordienko, D, Hastie, R, Oddos, T, *et al.* (2013). ORAI1 calcium channel orchestrates skin homeostasis. *Proc Natl Acad Sci USA* 110: E4839–48.
Wilson, SR, Thé, L, Batia, LM, Beattie, K, Katibah, GE, McClain, SP, *et al.* (2013). The Epithelial Cell-Derived Atopic Dermatitis Cytokine TSLP Activates Neurons to Induce Itch. *Cell* 155: 285–95.

FIGURE LEGENDS

Figure 1

Hypoosmotic stress induces IL-33 in primary human keratinocytes

Panels **a&b** show immunofluorescent stainings of human skin tissue for pSTAT1 (green) and nuclear marker Topro-3 (blue), dotted line marks dermo-epidermal junction. Panels **c - l** show keratinocytes exposed to isoosmotic, hypoosmotic or hyperosmotic medium and are examined by immunofluorescence (**c&d**) for IL-33 (red) and keratin 14 (green), by ELISA of cell lysates and western blot (**e**), and by RT-PCR (**f**). Panel **g** shows IL-33 induction verified by siRNA knockdown and western blot analysis. Panels **h - l** show mRNA expression of various pro-inflammatory mediators in hypo-, iso- and hyper-osmotic conditions examined by RT-PCR, data are shown as mean ± SD of three replicates *P⩽ 0.05; **P⩽ 0.01; ****P⩽ 0.0001 (increase vs isoosmotic); #P<0.05 (decrease vs isoosmotic); ns=non-significant.

Figure 2

Primary keratinocytes show an atypical morphological response to hypoosmotic shock

Panel **a** shows phase-contrast microscopy images of keratinocytes that were left exposed for 15 minutes in isoosmotic or hypoosmotic medium. Panels **b** & **c** show IL-33 ELISA data of keratinocytes exposed to hypoosmotic medium before returning to isoosmotic medium or vice versa (**b**) or exposed for 6 hours to medium diluted with 50% water, or 50% isoosmotic solutions of phosphate-buffered saline, potassium gluconate or sodium gluconate (**c**). ELISA data are shown as mean ± SD of three replicates. ****P ⩽ 0.0001 (increase vs. isoosmotic). Panel **d** shows western blot of IL-33 and tubulin after 6 hours of isoosmotic medium, hypoosmotic medium, isosmotic urea solution or isoosmotic sorbitol solution. Panel **e** shows cell morphology after 15 minutes of isoosmotic urea or sorbitol solution exposure.

Figure 3

Stress- or IFN-γ-induced IL-33 both depend on EGFR signaling but have different upstream mediators

In panel **a** keratinocytes were stimulated in normal growth medium with recombinant EGF or exposed to hypoosmotic medium with or without pre-incubation with EGFR tyrosine kinase inhibitor (AG1478) or anti-EGFR antibody (cetuximab) for 6 hours. In panel **b** keratinocytes were left in basal medium without growth factors 90 minutes before stimulations and subsequently exposed to hypoosmotic medium and/or different concentrations of amphiregulin for 6 hours. Panels **c**-**h** show immunofluorescence of IL-33 (greyscale, **c**-**e**) or combination (**f**-**h**) of IL-33 (red) and Ki67 (green) in keratinocytes that were either untreated, exposed to IFN-γ or to hypoosmotic stress. Panel **i** shows western blot of keratinocytes stimulated with either IFN-γ or hypoosmotic medium with different concentrations of pan-JAK inhibitor I.

Figure 4

Calcium-dependent processes drive IL-33 production and modulate the general pro-inflammatory response to hypoosmotic stress

Panel **a** shows IL-33 ELISA of keratinocyte lysates treated with calcium chelator BAPTA-AM before stimulation. Data are shown as mean ± SD of three replicates, ****P $\leqslant$ 0.0001. Panel **b** shows confluent keratinocytes switched to calcium-free medium and stimulated with IFN-γ or hypoosmotic solution, adding either 0.07 mM $CaCl_2$ (low calcium), EGTA, BAPTA-AM chelator or 1.2 mM $CaCl_2$ (high calcium). Panel **c** shows RT-PCR data of pro-inflammatory mediators from keratinocytes exposed to stressors with or without BAPTA-AM. Data represent fractions of maximum mRNA levels set to 100% within the four conditions. In panel **d** selected transcript levels from IL-33 siRNA-treated keratinocytes were

analyzed by RT-PCR. Data show mean fold change ± SD of three replicates. ns=non-significant, ***P ⩽ 0.001.

Figure 5

Hypoosmotic stress is a relevant tissue signal

Normal human skin tissue was either immediately fixed in formalin (**a**) or cultured *ex vivo* for 24 hours in normal medium (**b**), hypoosmotic medium (**c**) or with addition of IFN-γ (**d**) with subsequent formalin fixation. Sections of formalin-fixed paraffin-embedded tissue were stained with immunofluorescent technique for IL-33 (red), STAT-1 (green) and nuclear stain with Hoechst (blue). Single color images of the same stainings are shown for IL-33 (greyscale, **e-h**) and pSTAT (greyscale, **i-l**).

Figure 1

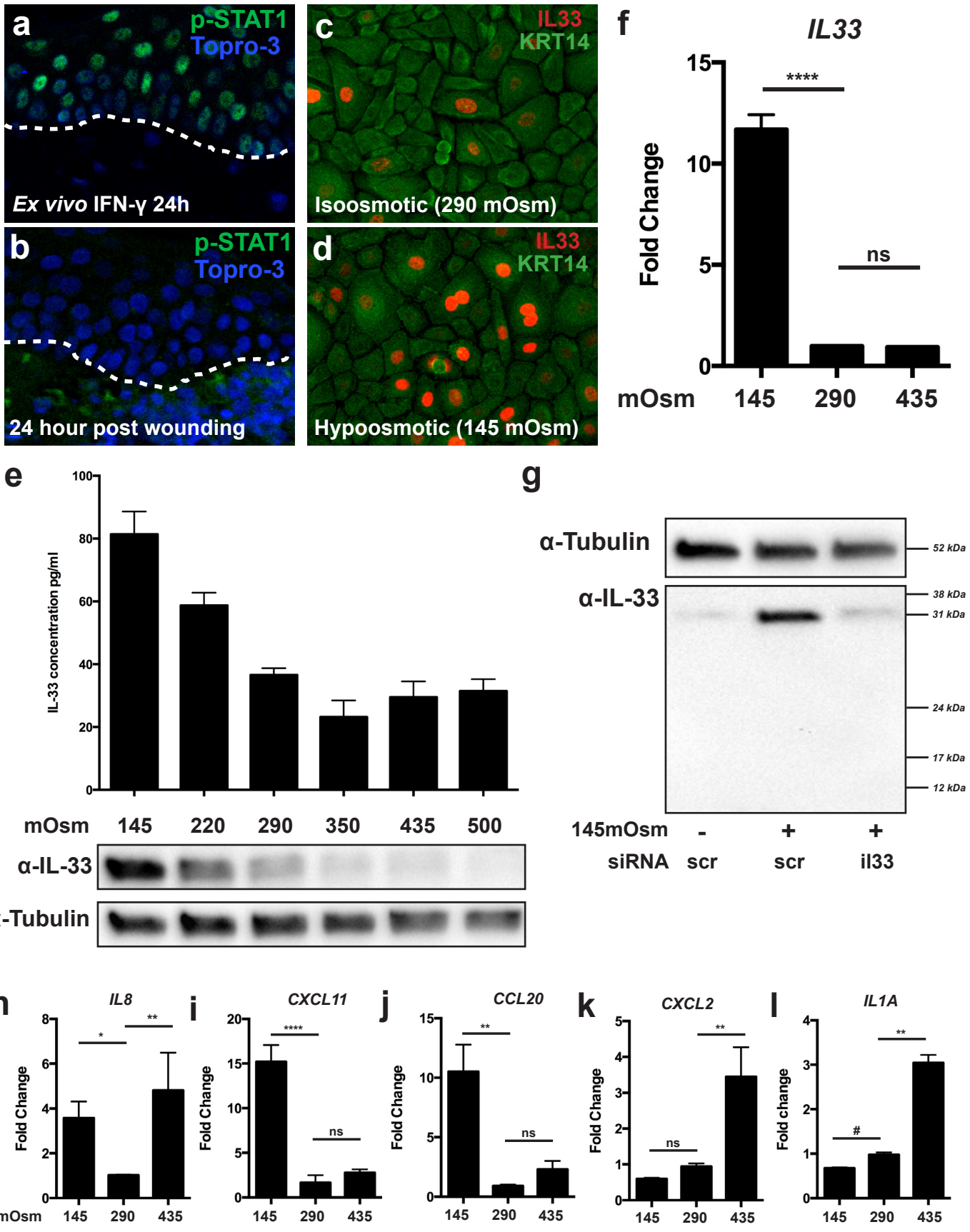
a
p-STAT1
Topro-3
Ex vivo IFN-γ 24h
b
p-STAT1
Topro-3
24 hour post wounding
c
IL33
KRT14
Isoosmotic (290 mOsm)
d
IL33
KRT14
Hypoosmotic (145 mOsm)
f
IL33
Fold Change
****
ns
mOsm 145 290 435
e
IL-33 concentration pg/ml
mOsm 145 220 290 350 435 500
α-IL-33
α-Tubulin
g
α-Tubulin
α-IL-33
52 kDa
38 kDa
31 kDa
24 kDa
17 kDa
12 kDa
145mOsm - + +
siRNA scr scr il33
h
IL8
i
CXCL11
j
CCL20
k
CXCL2
l
IL1A
Fold Change
Fold change
mOsm 145 290 435

Figure 2

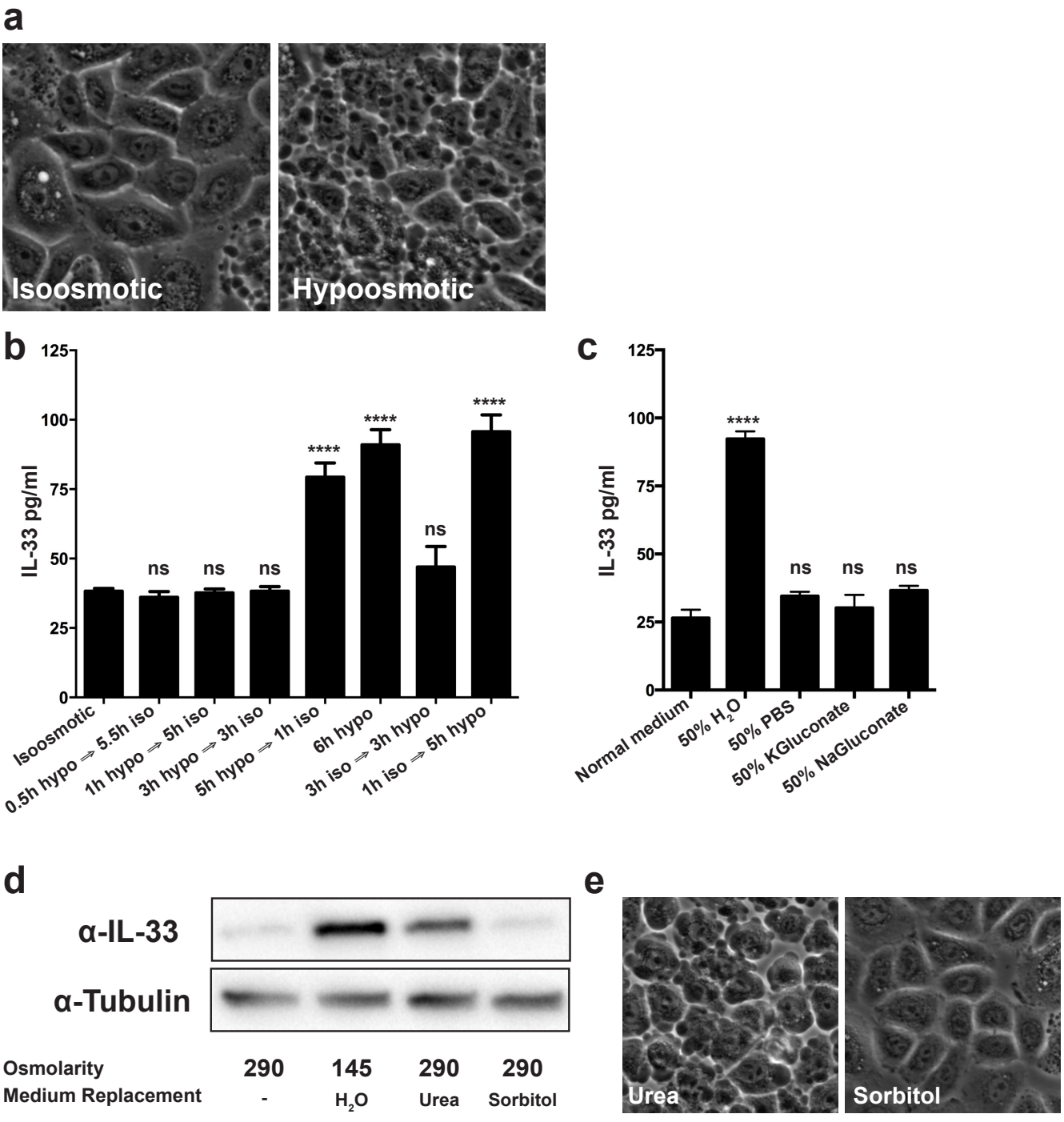
a
Isoosmotic
Hypoosmotic
b
IL-33 pg/ml
125
100
75
50
25
0
ns
ns
ns
****
****
ns
****
Isoosmotic
0.5h hypo ⇒ 5.5h iso
1h hypo ⇒ 5h iso
3h hypo ⇒ 3h iso
5h hypo ⇒ 1h iso
6h hypo
3h iso ⇒ 3h hypo
1h iso ⇒ 5h hypo
c
IL-33 pg/ml
125
100
75
50
25
0
****
ns
ns
ns
Normal medium
50% H2O
50% PBS
50% KGluconate
50% NaGluconate
d
α-IL-33
α-Tubulin
Osmolarity
Medium Replacement
290
-
145
H2O
290
Urea
290
Sorbitol
e
Urea
Sorbitol

Figure 3

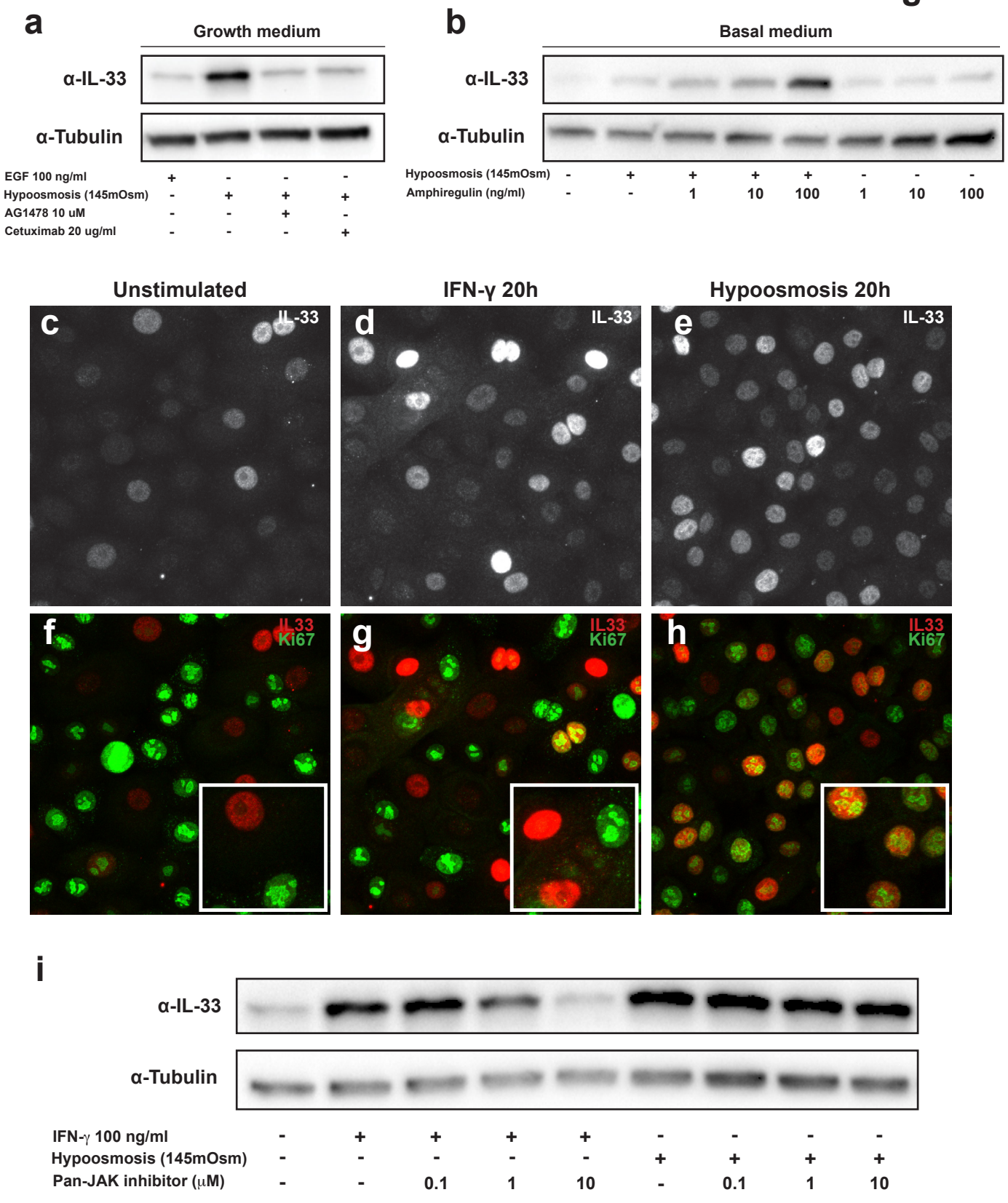
a
Growth medium
α-IL-33
α-Tubulin
EGF 100 ng/ml + - - -
Hypoosmosis (145mOsm) - + + +
AG1478 10 uM - - + -
Cetuximab 20 ug/ml - - - +
b
Basal medium
α-IL-33
α-Tubulin
Hypoosmosis (145mOsm) - + + + + - - -
Amphiregulin (ng/ml) - - 1 10 100 1 10 100
Unstimulated
IFN-γ 20h
Hypoosmosis 20h
c
IL-33
d
IL-33
e
IL-33
f
IL33
Ki67
g
IL33
Ki67
h
IL33
Ki67
i
α-IL-33
α-Tubulin
IFN-γ 100 ng/ml - + + + + - - - -
Hypoosmosis (145mOsm) - - - - - + + + +
Pan-JAK inhibitor (μM) - - 0.1 1 10 - 0.1 1 10

Figure 4

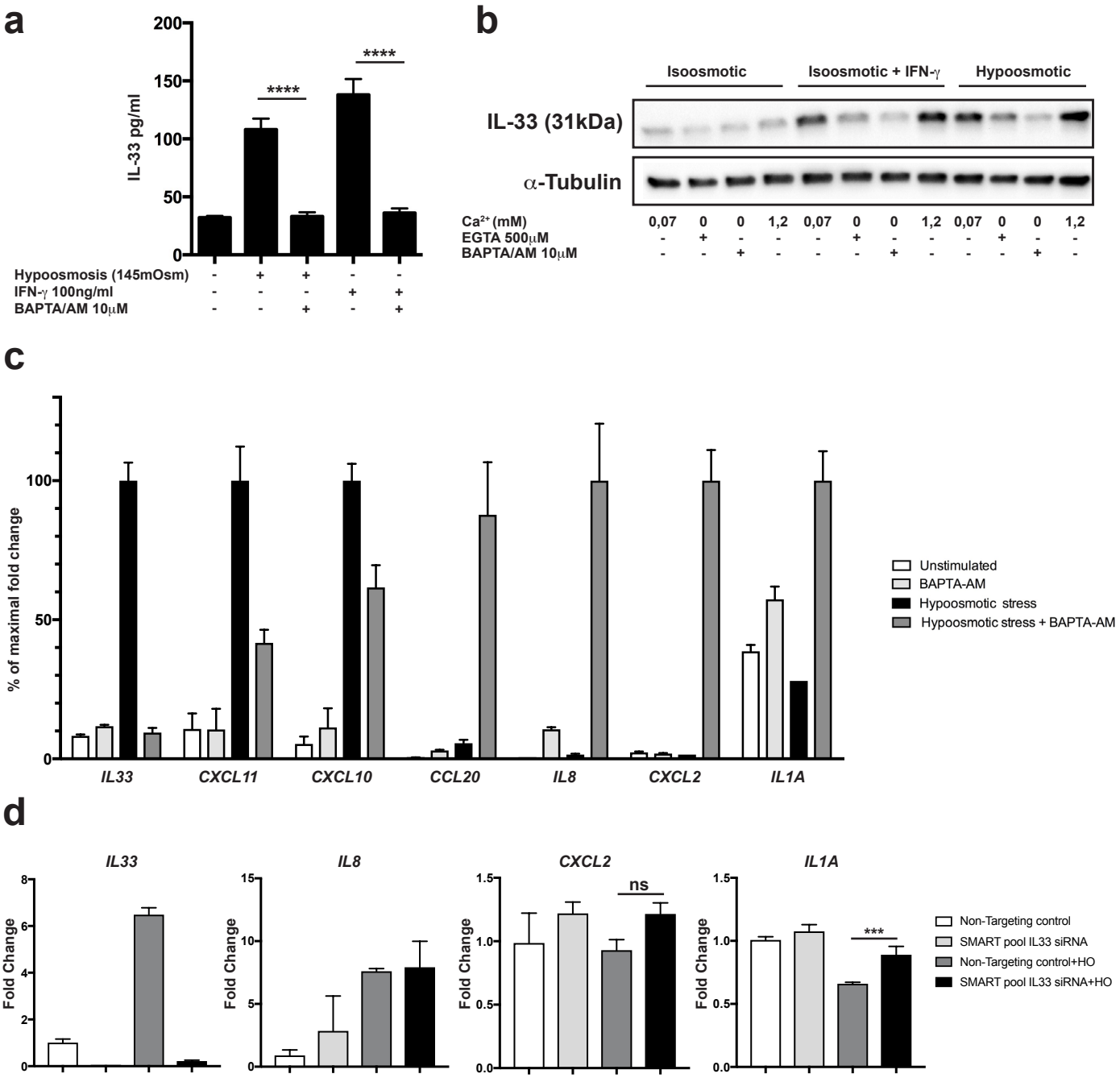
a
IL-33 pg/ml
200
150
100
50
0
****
****
Hypoosmosis (145mOsm) - + + - -
IFN-γ 100ng/ml - - - + +
BAPTA/AM 10μM - - + - +
b
Isoosmotic
Isoosmotic + IFN-γ
Hypoosmotic
IL-33 (31kDa)
α-Tubulin
Ca2+ (mM) 0,07 0 0 1,2 0,07 0 0 1,2 0,07 0 0 1,2
EGTA 500μM - + - - - + - - - + - -
BAPTA/AM 10μM - - + - - - + - - - + -
c
% of maximal fold change
100
50
0
IL33
CXCL11
CXCL10
CCL20
IL8
CXCL2
IL1A
Unstimulated
BAPTA-AM
Hypoosmotic stress
Hypoosmotic stress + BAPTA-AM
d
IL33
IL8
CXCL2
IL1A
Fold Change
ns
***
Non-Targeting control
SMART pool IL33 siRNA
Non-Targeting control+HO
SMART pool IL33 siRNA+HO

Figure 5

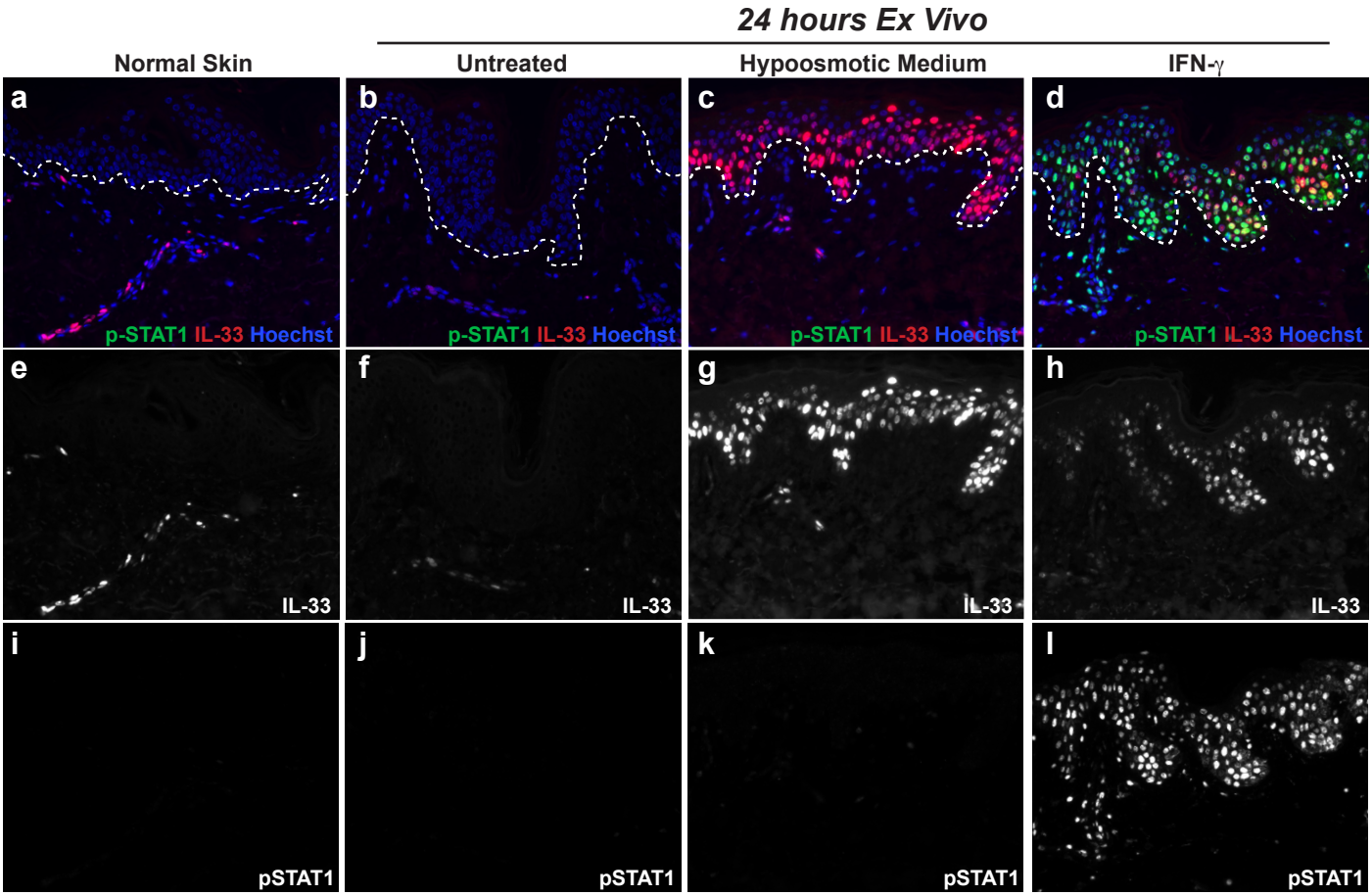
24 hours Ex Vivo
Normal Skin
Untreated
Hypoosmotic Medium
IFN-γ
a
b
c
d
p-STAT1 IL-33 Hoechst
e
f
g
h
IL-33
i
j
k
l
pSTAT1

SUPPLEMENTARY INFORMATION

Antibodies

Specificity	Designation	Working Concentration	Specification	Source
human IL-33	Nessy-1	IHC: 5 μg/ml WB: 1 μg/ml	Mouse IgG1	Enzo Life Science
Keratin 1	AF109	IHC: 2 μg/ml	Rabbit polycloncal	Covance
Keratin 14	D19-N	IHC: 0.15 μg/ml	Rabbit monoclonal	Abnova
Ki67	ab15580	IHC: 2.5 μg/ml	Rabbit monoclonal	Abcam
pSTAT1	58D6	IHC: 1/400	Rabbit monoclonal	Cell Signaling
α-tubulin	ab6046	WB: 2 μg/ml	Rabbit polycloncal	Abcam
STIM1	EPR3414	WB: 0.3 μg/ml	Rabbit monoclonal	Abcam

Primer sequences

Gene	Forward	Reverse
IL33	5'-TGTCAACAGCAGTCTACTGTGGAGTGCT-3'	5'-GCAAAAGTAATGGATTGATCATTGTA-3'
CXCL10	5'-GTGGCATTCAAGGAGTACCTC-3'	5'-TGATGGCCTTCGATTCTGGATT-3'
CXCL11	5'-TGTCTTTGCATAGGCCCTGG-3'	5'-TAAGCCTTGCTTGCTTCGAT-3'
IL8	5'-ACAAGAGCCAGGAAGAAACC-3'	5'-GGCAAAACTGCACCTTCACA-3'
CXCL2	5'-CGCCCAAACCGAAGTCATAG-3'	5'-GCCATTTTTCAGCATCTTTTCG-3'
IL1A	5'-GTCAGCAAAGAAGTCAAGATGGC-3'	5'-CATGGAGTGGGCCATAGCTT-3'
HPRT	5'-AATACAAAGCCTAAGATGAGAGTTCAAGTTGAGTT-3'	5'-CTATAGGCTCATAGTGCAAATAAACAGTTTAGGAAT-3'
B2M	5'-TGCTGTCTCCATGTTTGATGTATCT-3'	5'-TCTCTGCTCCCCACCTCTAAGT-3'

Osmolarity measurement

The osmolarity of the CnT-57 culture medium was measured to be approx. 290 mOsm (+/- 5 mOsm) with a Fiske One-Ten Osmometer, and this value corresponded to the specification of the medium given by the producer. Consequently, all experiments were based on an isosmolarity of 290 mOsm. To induce hypoosmotic stress half of the medium was replaced with sterile water, and for hyperosmotic stress a 10X NaCl (2900 mOsm) solution was diluted to desired osmolarity adjusted for a further dilution in half volume of culture medium. For experiments with urea, sorbitol, potassium gluconate and sodium gluconate the substances were dissolved in sterile water to achieve 290 mOsm and added to replace half the volume of the culture medium.

RNA interference

Subconfluent NHEKs, cultured in a 12-well plate format, were washed twice with sterile PBS and each well was transfected for 6 hours with SMARTpool: ON-TARGETplus IL33 siRNA or ON-TARGETplus Non-targeting Pool (final conc. 25nM, Dharmacon) along with 4 µl of lipofectamine RNAiMAX (Invitrogen) according to the manufacturer's instructions. Transfection was performed in a basal antibiotic-free keratinocyte medium (CnT-BM.1, CELLnTEC) for 6 hours. After transfection, NHEKs were placed in normal keratinocyte growth medium (CnT-57.S, CELLnTEC) with antibiotics, cultured for 72 hours to reach confluence and exposed to hypoosmotic medium for 6 hours.

Human tissues, human skin wounding model and ex vivo organ culture

For the organ culture model eight milimeter punch biopsies of normal human skin was incubated in Millicell PCF 12 mm culture inserts (Millipore) in 12-well plates filled with culture medium (DMEM (Carlsbad, CA) supplemented with 10% fetal calf serum and 100

U/ml Penicillin & 100 µg/ml Streptomycin) to the level of the epidermis for 24h. For hypoosmotic stimulation half of the volume of medium was replaced with sterile water and for IFN-γ stimulation the cytokine was added at concentration of 100 ng/ml to the culture medium. Samples were then formalin-fixed and processed for immunohistochemistry.

Western Blot

Keratinocytes grown and stimulated in 12-well plates were lysed in SDS lysis buffer (as described previously (Grøvdal et al., 2004)) containing protease inhibitor cocktail (Sigma) and phosphatase inhibitor cocktail 2 (Sigma). Samples were homogenized using QIAshredder (Qiagen) columns, according to manufacturer's protocol. Western Blotting was performing using 10% Mini-PROTEAN®TGX™ Precast Gels (Bio-Rad), Trans-Blot® Turbo™ Mini Nitrocellulose Transfer Packs (Bio-Rad Laboratories) and Trans-Blot® Turbo™ Transfer System (Bio-Rad Laboratories). Membranes were then immunoblotted with primary antibodies followed by secondary HRP-conjugated detection antibodies. Immunoreactive proteins in cell lysates were detected using SuperSignal West Dura Extended Duration Substrate (Thermo Fischer Scientific, Waltham, MA) and visualized using the ChemiDoc MP System (Bio-Rad Laboratories, Hercules, CA).

Live Imaging

Cells were grown on 2-well or 8-well µ-slide with ibiTreat (Ibidi) and placed on the stage of a Zeiss Axiovert 100 inverted microscope fitted with a Solent Scientific (Segensworth, UK) incubation chamber (37°C) and a HQ CoolSnap digital camera (Photometrics, Ottobrunn, Germany) and time-lapse image series were acquired using the MetaMorph 7.5.3 software (Molecular Devices, Silicon Valley, CA).

Immunohistochemistry and immunocytochemistry

Sections (3 μm) of formalin-fixed, paraffin-embedded samples were mounted to Superfrost Plus slides (Menzel-Gläser, Braunschweig, Germany) and processed and stained by a Ventana Discovery Ultra staining robot (Ventana, Tuscon, AZ) or processed and stained manually. Manual procedure included deparaffinized before antigen retrieval in Target Retrieval Solution (Dako, Copenhagen, Denmark, pH6) at 100°C (20 min) in a water bath. Blocking was performed with 5% donkey serum (20 min) before slides were incubated with primary antibodies overnight (4°C) followed by fluorescent detection with Alexa-conjugated secondary antibodies (Invitrogen). Nuclear staining was performed with Hoechst or Topro-3 as indicated. Cells were cultured on LabTek 8-well chamber slides (Thermo Fisher Scientific, Rochester, NY) and fixed with 4% PFA. All antibodies were incubated with 0.1% saponin for permeabilization. Primary antibodies were incubated overnight at 4°C, and secondary Alexa-conjugated antibodies were incubated for 2 hours at 20°C. Images were generated either with a Zeiss 510Meta Confocal Microscope with Zen software or with a Nikon Ellipse E800 widefield microscope equipped with Nikon Plan-Fluor objectives and either an F-VIEW digital camera controlled by AnalySIS 3.2 software (Soft Imaging System) or a Zeiss Axiocam MRm camera with Zen software.

ELISA

Keratinocytes were grown to confluence and stimulated in 12-well plates and lysed in 200 uL of M-PER lysis buffer (Thermo Fischer Scientific, Waltham, MA) supplemented with protease inhibitor cocktail (Sigma, St. Louis, MO). Lysates were analysed with human IL-33 DuoSet ELISA (R&D Systems, Minneapolis, MN) according to the manufacturer's protocol. Absorbance was recorded with an Epoch microplate reader (BioTek, Winooski, VT).

RT-PCR

RNA was isolated from keratinocytes using TriReagent (Life Technologies) according to the manufacturer's instructions. Total RNA was reverse-transcribed using Oligo(dT) and SuperScript III Reverse Transcriptase (Life Technologies). Gene transcripts were quantified by real-time quantitative PCR (qPCR) using a Stratagene Mx3005P system (Agilent Technologies, Santa Clara, CA). Transcript levels of target genes were normalized against transcript levels for hypoxanthine-guanine phosphoribosyltransferase (*hprt*) or (*b2m*). Primer sequences are given in separate table.

Supplementary figure legends

Figure S1

Western blot of IL-33 and tubulin taken from lysed confluent human umbilical vein endothelial cells (HUVECs) left in normal medium or exposed to medium where 30% or 50% of medium was replaced with water (**a**).

Figure S2

In panel **a** confluent culture of primary human keratinocytes was exposed to hypoosmotic medium and pictures of phase-contrast time-lapse photography were taken for different time-points. Panel **b-e** show immunostainings of IL-33 and Keratin 14 (KRT14) in a confluent keratinocyte culture exposed for 6h to isoosmotic medium (**b**), hypoosmotic medium (**c**), Latrunculin A in isosmotic medium (**d**) and Latrunculin A in hypoosmotic medium (**e**). Panel **f** shows phase-contrast photography of confluent keratinocyte culture before addition of Latrunculin A and 1.5 min after addition. In panel **g** lysates of keratinocytes pre-incubated for 30 minutes with Latrunculin A and cultured for additional 6 hours in normal growth medium or in hypoosmotic medium were analyzed by Western blot for IL-33 and tubulin. Panel **h** & **i**

show IL-33 ELISA data and Western blot of keratinocytes exposed to hypoosmotic medium for 6 hours with or without pre-incubation with caspase-1 inhibitors Z-WEHD-FMK and Caspase-1 inhibitor IV. ELISA data are shown as mean ± SD of three replicates and are representative of 1-3 independent experiments. ns=non-significant.

Figure S3

Immunofluorescence stainings for IL-33 (red), Keratin 1 (green) and nuclear marker Topro-3 (blue) are shown in panels **a** & **b**. Normal human keratinocytes were grown to confluence and either continued in low calcium proliferation medium (**a**) or changed to differentiation medium for 48 hours with added 1.2 mM $CaCl_2$ the last 24 hours for complete differentiation (**b**). Panel **c** shows images from time-lapse microscopy of cells pre-incubated with BAPTA-AM for 30 minutes and then exposed to hypoosmotic medium at time=0 and followed for 5 hours. In panel **d-j** the same data presented in figure 4c are shown for individual genes with the fold change of the respective gene relative to housekeeping gene *HPRT*. PCR data are shown as mean ± SD of three replicates. ***P $\leqslant$ 0.001, ****P$\leqslant$ 0.0001

Figure S4

Keratinocyte lysates were analyzed by either IL-33 ELISA (**c** & **d**) or Western blot for IL-33 and tubulin (**a**, **b**, **e** & **f**) after stimulation for 6 hours with hypoosmotic medium with or without 30 minutes pre-incubation with BAPTA-AM (10 μM), STIM1 inhibitor SKF9365 (10μM) and STIM-1-ORAI inhibitor ML-9 (10 μM), TRP blocker Ruthenium Red (10 μM), L-type calcium channel blockers Verapamil (10 μM) or Nifedipine (100 μM), purinergic inhibitor Suramin, ATP-degrading enzyme Apyrase or different concentrations of PLC-γ inhibitor U73122. In **b** keratinocytes were transfected with either scrambled, IL-33 or four different STIM1-specific siRNAs, grown to confluence for 72 hours and stimulated for 6

hours with hypoosmotic medium. Western blot of cell lysates was performed for STIM1, IL-33 and tubulin. ELISA data are shown as mean ± SD of three replicates, ns= non-significant.

a

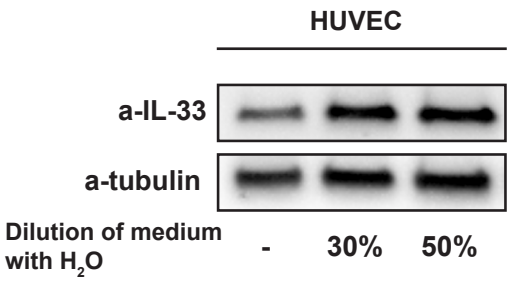

Figure S2

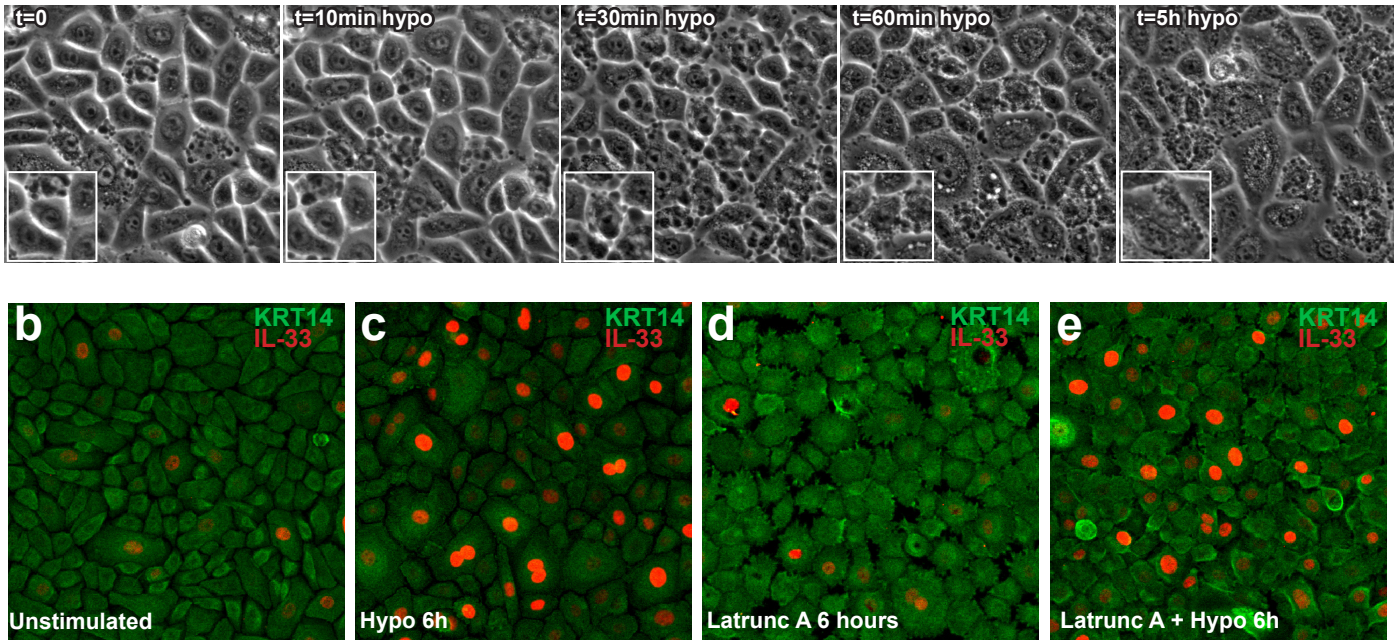
a
t=0
t=10min hypo
t=30min hypo
t=60min hypo
t=5h hypo
b
KRT14
IL-33
Unstimulated
c
KRT14
IL-33
Hypo 6h
d
KRT14
IL-33
Latrunc A 6 hours
e
KRT14
IL-33
Latrunc A + Hypo 6h

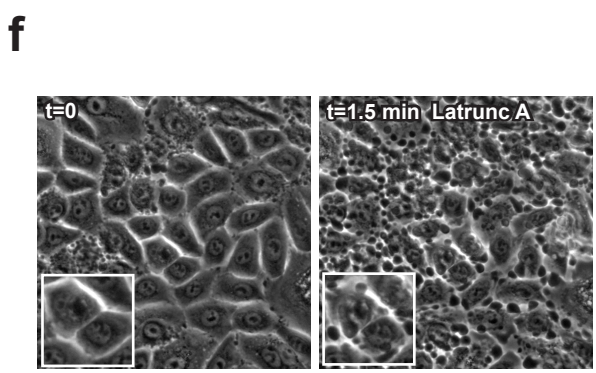
f
t=0
t=1.5 min Latrunc A

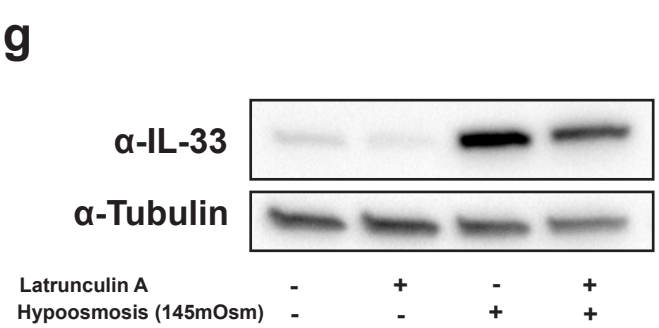
g
α-IL-33
α-Tubulin
Latrunculin A - + - +
Hypoosmosis (145mOsm) - - + +

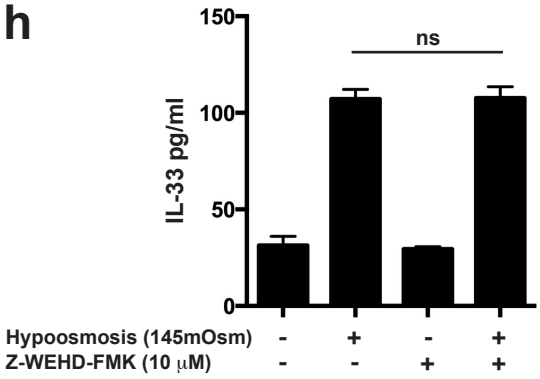
h
150
100
50
0
IL-33 pg/ml
ns
Hypoosmosis (145mOsm) - + - +
Z-WEHD-FMK (10 μM) - - + +

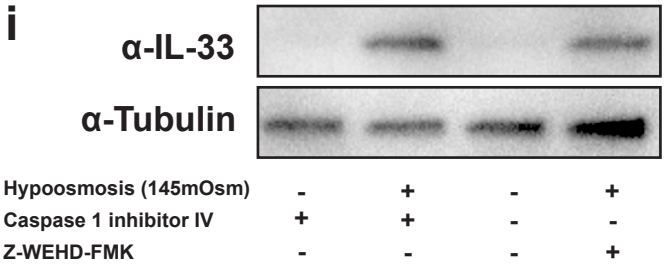
i
α-IL-33
α-Tubulin
Hypoosmosis (145mOsm) - + - +
Caspase 1 inhibitor IV + + - -
Z-WEHD-FMK - - - +

Figure S3

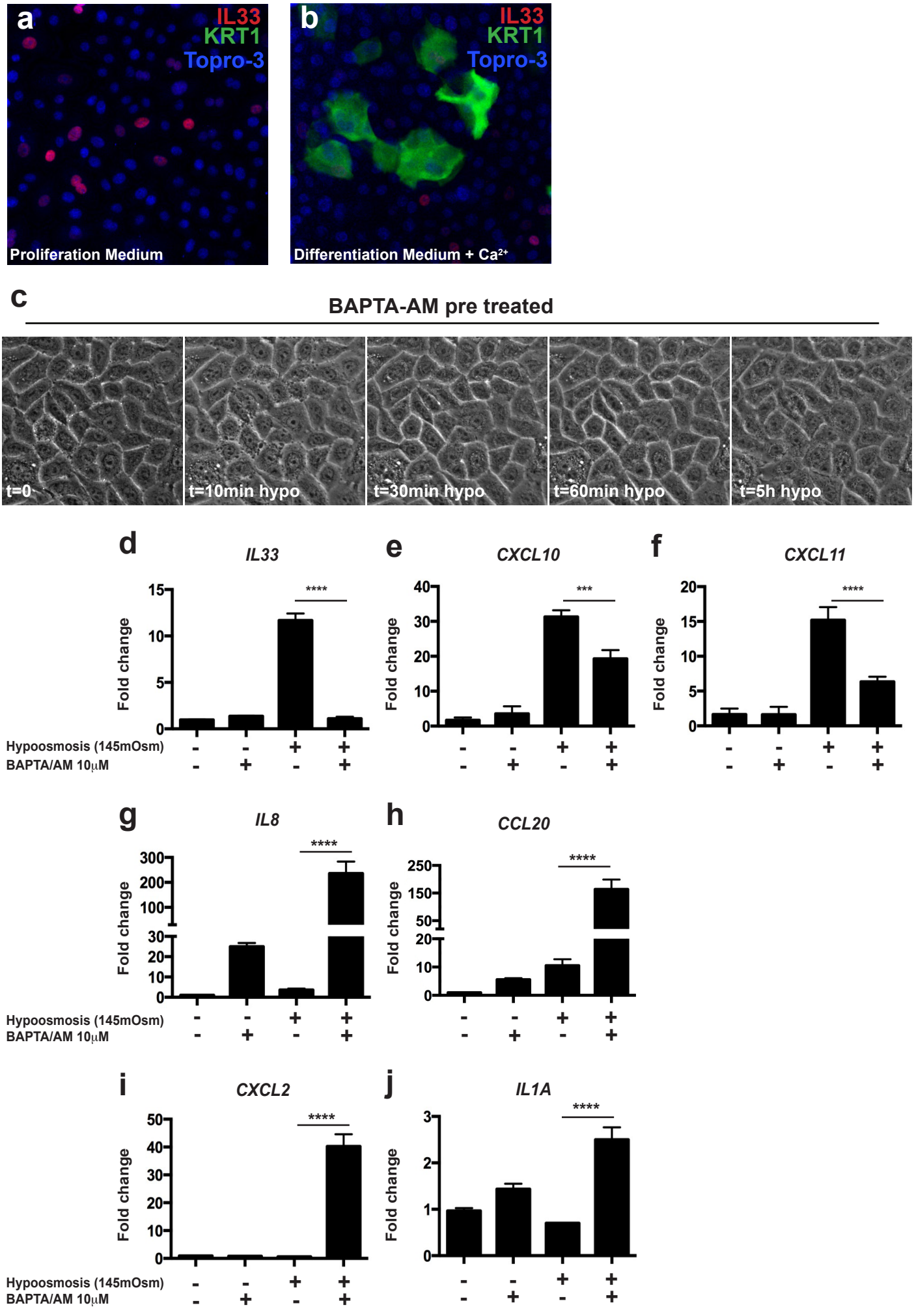
a
IL33
KRT1
Topro-3
Proliferation Medium
b
IL33
KRT1
Topro-3
Differentiation Medium + Ca2+
c
BAPTA-AM pre treated
t=0
t=10min hypo
t=30min hypo
t=60min hypo
t=5h hypo
d
IL33
e
CXCL10
f
CXCL11
g
IL8
h
CCL20
i
CXCL2
j
IL1A
Fold change
Hypoosmosis (145mOsm)
BAPTA/AM 10μM
****
***

Figure S4

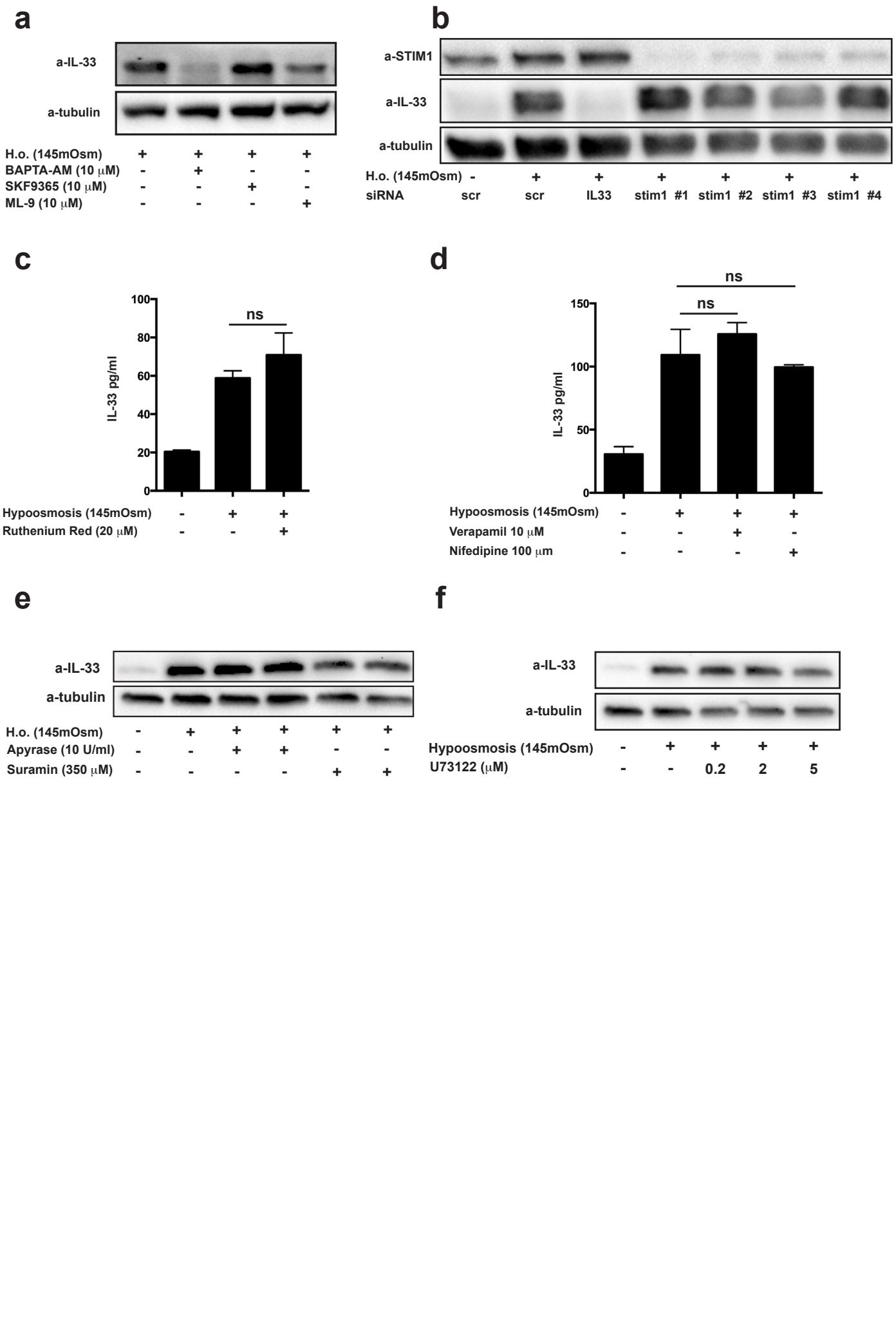
a
a-IL-33
a-tubulin
H.o. (145mOsm) + + + +
BAPTA-AM (10 μM) - + - -
SKF9365 (10 μM) - - + -
ML-9 (10 μM) - - - +
b
a-STIM1
a-IL-33
a-tubulin
H.o. (145mOsm) - + + + + + +
siRNA scr scr IL33 stim1 #1 stim1 #2 stim1 #3 stim1 #4
c
IL-33 pg/ml
100
80
60
40
20
0
ns
Hypoosmosis (145mOsm) - + +
Ruthenium Red (20 μM) - - +
d
IL-33 pg/ml
150
100
50
0
ns
ns
Hypoosmosis (145mOsm) - + + +
Verapamil 10 μM - - + -
Nifedipine 100 μm - - - +
e
a-IL-33
a-tubulin
H.o. (145mOsm) - + + + + +
Apyrase (10 U/ml) - - + + - -
Suramin (350 μM) - - - - + +
f
a-IL-33
a-tubulin
Hypoosmosis (145mOsm) - + + + +
U73122 (μM) - - 0.2 2 5